Single-phase Multi-component Simulation of RBCs Biconcave Shape Using 2-D Lattice Boltzmann Method

H. Farhat, J.S. Lee

Multi-scale Fluid Dynamics laboratory. Department of Mechanical Engineering.
Wayne State University, Detroit, MI 48202.

ABSTRACT

The dependence of the rheological properties of blood, on RBCs shape, aggregation and deformability has been investigated using hybrid systems which couple fluid with solid models [1-4]. We are presenting a simplistic approach for simulating blood as a multi-component fluid, in which RBCs are modeled as droplets of acquired biconcave shape. We use LBM, owing to its excellent numerical stability as a simulation tool. The model enables good control of the droplet shape by imposing variable surface tension on the interface between the two fluids. The use of variable surface tension is justified by Norris hypotheses, which was supported by recent experiments. This hypotheses states that the shape of the erythrocytes is due to a difference in surface tension caused by the unbalanced distribution of lipid molecules on the surface [5].

Keywords: blood rheology, rbc deformability, rbc shapes, lbm.

1 INTRODUCTION

Biconcave shape and deformability have major influence on the red blood cell delivery functions. Erythrocyte's shape provides higher surface to volume ratio. This is believed to have crucial role in the gas exchange process, which takes place in the body, and especially in the lungs and the periphery [5]. Deformability allows red blood cells to circulate inside microvessels having dimension about half of their size.

Shape and deformability are the subjects of many studies. Of the currently available explanations to these phenomena, two distinct hypotheses are considered.

1.1 Minimal Energy Hypotheses

Classic Canham-Helfrich hypothesis, suggests that the biconcave equilibrium shape of erythrocytes, results from the requirement of minimization of the total bending energy [6].

More recent studies show that the cytoskeleton undergoes constant remodeling in its topological connectivity, in order to achieve zero in plane shear elastic energy [7].

The main goal is to simulate the spectrin network remodeling process and fluidization, and to highlight the network influence on the shape and deformability of the erythrocytes. Spectrin network is modeled as spherical beads connected by unbreakable springs. In some cases thermal and biochemical factors are considered, but hydrodynamic interactions are ignored [7].

The inherent problem of these models, is that the biconcave shape is hardly achieved by carefully selecting the stress-free reference state otherwise cup shape is the dominant [6].

Other models use hybrid systems, which couple the solid model with fluid model. The biconcave shape is achieved by minimizing the total elastic energy of the solid model [4], or by using analytical formula [2].

Generally these models focused on the deformability of the cells during blood motion but failed to recognize the role of the quiescent fluid on the erythrocyte's shape.

1.2 Surface Tension Hypotheses

Surface tension hypothesis suggests that the shape of the erythrocyte is caused by the balance between the spreading tendencies of the lipid molecules of the cell, counteracted by the surface tension forces which cause a fluid object to become spherical in shape, when immersed into another fluid [5].

Experiments using radio autography, shows that labeled cholesterol incorporated into the cell membrane, was concentrated in the periphery of the biconcave disk, while little were found in the flat central area of the erythrocyte [5]. These experiments indicate that the erythrocyte's lipid bilayer is concentrated at the peripheries, which makes these areas less wet-table with corresponding higher surface tension interfacial forces [5].

This theory is further supported by the fact that some substances like bile, free fatty acids, lysolecithin and saponinc; transform the erythrocyte into a sphere, when interacting with it. This process is totally reversible. Washing the spherical RBC with plasma turns it back into its original biconcave shape [5].

Two important facts are worth mentioning about this theory. The first is about the minimal stretching ability of the cytoskeleton as contrasted with its deformability. Since the red blood cell surface area is almost maintained during deformation, it requires less energy from the flow to pass through microvessels. No energy is wasted to stretch the membrane. The second circulation energy saving comes from the fact that the shape of the red blood cell results from the physical interaction between the plasma and the membrane and not from the flow circulation [5].

Another support of this hypothesis comes from fact that red blood cell lipids form immiscible fluid under pressure of

21 dyn/cm for the inner leaflet, and 29 dyn/cm for the outer leaflet [8].

In this paper we are exploring the possibility of using surface tension hypotheses, to answer some basic questions, like the origin of the biconcave shape, and blood cell deformability, but the longer term aim is to try to map the topology of the lipid bilayer during deformation in order to understand the dynamics of this process.

2 NUMERICAL METHOD

Multi-component lattice Boltzmann simulation is a convenient tool for modeling blood under surface tension hypotheses. We use D2Q9, two-components, isothermal, single relaxation, LBGK model. We use guidance from [9], and follow the footsteps of I. Halliday et al [10-12], who did an extensive work to improve the models by Gunstensen et al [13], D'Ortona et al [14], and Listchuk et al [15].

We identify the red and blue fluids momentum distribution functions as $R_i(r,t)$, and $B_i(r,t)$, where *r* and *t* are the nodal position and time respectively. The nodal density of the two fluids is defined individually.

$$R(r,t) = \sum R_i(r,t) \quad (1)$$

$$B(r,t) = \sum B_i(r,t) \quad (2)$$

The total momentum distribution function is the sum of the two functions.

$$f_i(r,t) = R_i(r,t) + B(r,t) \quad (3)$$

The main streaming and collision function is the single particle model and is expressed as follows.

$$f_i(r + c_{i,}t + 1) = f_i(r,t) - \omega[f_i(r,t) - f_i^0(\rho,\rho u)] + \emptyset_i(r) \quad (4)$$

$\emptyset_i(r)$ is a forcing term and it is used to include a controlled body force in order to have an interfacial pressure step in the fluid [12]. Another term could be included to enclose a force in the horizontal direction, which causes fluid circulation.

The main idea in two-component LBM is to modify the collision rules, in order to obtain surface tension between the two fluids. This is achieved by applying two-step collision rules. The first step is done by the addition of perturbation to the particle distribution near the interface to create the correct surface-tension dynamics. The second step is the segregation of the two fluids by imposing zero diffusivity of one color into the other [12].

To define the interface between the two fluids a phase field is described as follows.

$$\rho^N(r,t) = \frac{R(r,t) - B(r,t)}{R(r,t) + B(r,t)} \quad (5)$$

In this model we follow Lischuk's interface method [15] where *N* stands for normal. A surface tension force F(r) is defined.

$$F(r) = -\frac{1}{2}\alpha K \nabla \rho^N \quad (6)$$

Notice that $\nabla \rho^N = 0$, for constant phase field. This means that this force is only applicable on the interface. α is a surface tension parameter. K is the curvature in the phase field, and is obtained from the surface gradients by finite difference method.

F(r) is used to correct the velocity following Guo's methodology [9] as shown in the following equation.

$$u^* = \frac{1}{\rho}(\mathrm{f_i c_i} + (1 - \mathrm{f})\mathrm{F(r)}), \quad \mathrm{f} = \frac{1}{2} \quad (7)$$

The first collision is then applied with the corrected velocities, followed by perturbing the interface using Gusntensen et al [12] perturbation term.

$$c_i^b = \alpha |\nabla \rho^N| \cos 2(\theta_i - \theta_f) \quad (8)$$

The binary collision operator c_i^b depletes mass along lattice links parallel to the interface and adds mass to lattice links perpendicular to it. θ_i is the angle of lattice direction i, θ_f is the angle of the local gradient.

The second collision step is segregation of the two components. The outcome is a solution to a maximization problem with two constraints of which one is.

$$B_i(r,t) = f_i(r,t) - R(r,t) \quad (10)$$

Segregation could be executed numerically as used by Gunstensen et al [12], or by using a set of formulae as described by the model of D'ortona et al [9].

After segregation the two components propagate individually. In our model we use numerical segregation.

3 SIMULATION RESULTS AND DISCUSSION

3.1 Biconcave Shape

The goal in this simulation was to show the surface tension hypotheses in action. We chose for demonstration in Fig.1, 60x60 lattices to model quiescent flow with periodic boundary condition in both directions, and without forcing term to cause circulation. We ran two simulations, first with

one droplet corresponding 10 % hematocrit, and second with two droplets, which corresponds to 20% hematocrit. Since the number of lattices determines the magnitude of the fluid body force, and therefore the surface tension as explained in part 2, we expect to use two different set of surface tension parameters and geometry for the two experiments.

The code optimized the variables in order to achieve the required shape and dimensions by running a loop with preset limits for these variables. The program stopped when the ratio stated in table 1 were within a preset range.

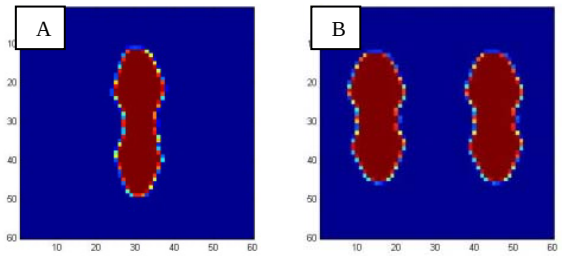

Figure 1: (A) Phase field contour for one cell, (B) for two cells. This figure shows the deformation of the droplets from square to biconcave shape under the influence of interfacial tension force. The only force applied on the two fluids is the controlled body force responsible for creating surface tension on the interface. There is no fluid flow in this simulation beside marginal micro-currents around the interface.

Condition	R1	R2	R3	R4
A	2.8	1.470	0.51	1.44
B	2.25	1.474	0.57	1.285
RBC	3.4	2.5	0.7	2.4

Table 1: R1is the ratio of the RBC length to width. R2 is the ratio of the RBC maximum width to the minimum width. R3 is the ratio of the initial length to final length, and R4 is the initial width to final width. In the case of real RBC the spheroid dimension is 6 µm as stated in [5].

The surface area and the mass of the RBC were conserved during this process. Using the right set of parameters, the droplet would take less than 10000 time steps to acquire its final shape. We used sigma scan pro for measurements. The results could improve if we increase the number of lattices, and widen the scope of the optimization parameters, but this will increase the computational cost.

3.2 Fahraeus-Lindqvist Effect

With a length of 26 lattices for the RBC, 100x60 lattices were used to demonstrate the physical basis of the Fahraeus-Lindqvist effect Fig.2. This effect predicts that the apparent viscosity of blood in long narrow vessels of diameter ranging from 7 µm up to 200 µm, tend to decrease with decreasing diameter. This is due to the presence of a cell- free layer, referred to as plasma-skimming layer near the wall.

Periodic conditions were applied on the vertical boundaries to create a resemblance of the condition of a long tube, and bounce back on the horizontal boundaries, to impose zero velocity on the wall as described in the theory [17].

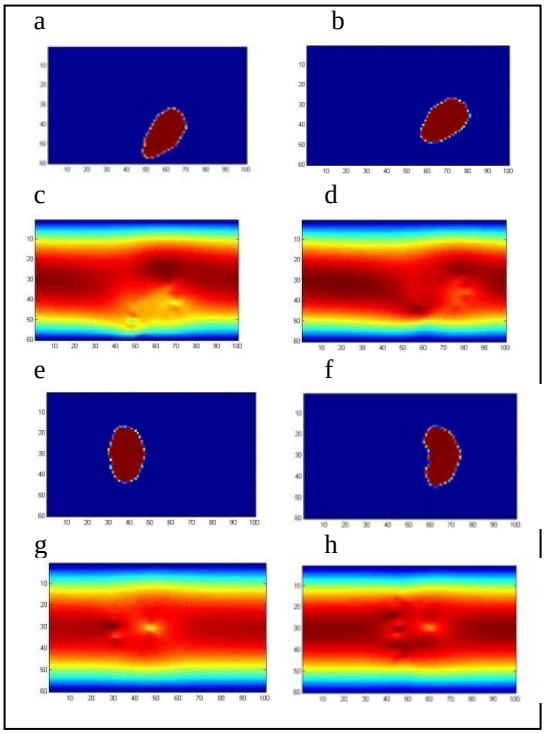

Figure 2: (a, b, e, f) Phase field contours for time steps 5, 8000, 22000, 300000 respectively. (c, d, g, h) Their respective horizontal velocity contour profiles. Looking at the velocity profile and considering subsonic flow conditions, one should consider higher pressure below the droplet, and lower pressure above it. This difference in pressure is responsible for the lift, which drives the droplet towards the center. When the droplet gets to the center, the pressure difference ceases to exist and the lift force vanishes.

This simulation clearly demonstrated in accordance with the theory [17], the tendency of the cell to rotate due to the viscous effects of the wall, and to migrate toward the center because of the Bernoulli force, as evident from the velocity profile.

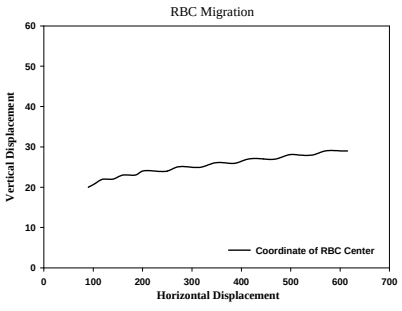

Figure 3: The graph shows the migration of the RBC towards the vertical center of the field. It takes about 30000 time steps for the cell to stabilize and move in a straight line at the center.

3.3 Fahraeus Effect

With a length of 26 lattices for the RBC, 100x60 lattices were used to demonstrate the Fahraeus effect Fig.3. This effect describes the fact that for small tubes, the hematocrit of the tube is smaller than the discharge hematocrit. This is because the RBC mean velocity is higher than the mean blood velocity.

We chose this frame because it corresponds to 20μm tube diameter simulation, which results were shown in [15]. Periodic conditions are applied on the vertical and bounce back on the horizontal boundaries. The mean velocity of the plasma was calculated by averaging all nodal velocities, after separating the RBC velocities from the data. The mean plasma velocity was found to be 0.0372 lu/ts, as compared to 0.0516 lu/ts for the RBC. The ratio of these velocities is 0.72, which is in agreement with the in vitro data recorded by Secomb (2003), and used for validating the model in [16]. We ran another experiment with 100x30, which corresponds to a tube with about 10 μm diameters. We found the plasma mean velocity to be 0.0175 lu/ts, and RBC mean velocity of 0.023lu/ts, giving a ratio of 0.75, which we could not confirm with experimental data.

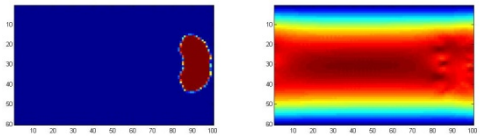

Figure 4: Phase field contour and horizontal velocity profile for 100x60 lattice frames. When the droplet moves in the centre of the flow a Poiseuille condition prevails. This means that the nodal velocities at the center of the flow and especially these of the droplet, will be higher than those of other regions.

3.4 RBC Deformation

100x24 lattices were selected randomly with forcing term of 2.75 E-5 corresponding Re 1.15 to qualitatively demonstrate the capability of the model to simulate variety of shapes resulting from the proximity of the RBC to the wall Fig.4. The objective was to mimic real time shapes obtained from pictures in a rat mesentery [18].

Comparing the simulation results with the real time pictures proves that treating RBC as droplet is more accurate than modeling it as linked springs. No flexible solid model could under real conditions deform in a way, similar to what we were seeing in the pictures. Based on our observation from this simulation we hypothesize that RBC deformation was not caused only by the rigidity of the wall, but rather mainly by the near wall fluid viscous effect. The droplet tends to take a bullet shape in short time after deforming in the vessel. This is due to the fact that the total area and mass of the droplet were conserved, and due to the nature of the flow velocity profile. The forehead of the droplet acquired higher momentum, which led to the formation of bullet shape, thereby spacing the droplet from the walls. This was associated with a reduction in the walls viscous effects, and a loss of the parachute tails. The droplet flow in the microvessels was enhanced. Careful observation of the real pictures shows a gap between the wall and the RBCs. It is worth mentioning that this hypothesis poses a real challenge to be experimentally proven.

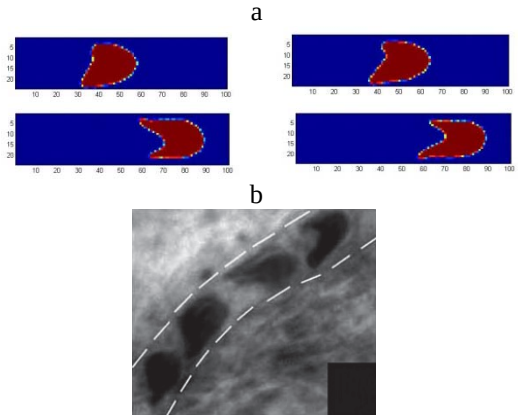

Figure 4: (a) Simulation results. (b) Real time picture of RBC in a rat mesentery**.** The resemblance of the simulation is quite good, because we picked up snap shots from three different simulations, for which the difference was only with the initial droplet position. One was central; the other was offset toward the bottom of the wall, while the last was offset toward the upper side of the wall.

We enclose a summary of the flow conditions of our simulations in Tab. 2.

Case No	Flow Re	Horizontal BC	Vertical BC
1	0	Periodic	Periodic
2	0.3	Bounce back	Periodic
3	0.15	Bounce back	Periodic
4	1.15	Bounce back	Periodic

Table 2: Flow conditions description for the four mentioned simulations

4 CONCLUSION

We are presenting a two dimensional two-component LBM model, which uses the surface tension hypotheses to explain the reason why biconcave discoid is the resting shape of RBC. The control parameters used to obtain the static shape of the erythrocyte are the same parameters, which we manipulate to control the shape of the red blood cell while streaming through microvessels. It is the author's intention to track the dynamic change in the lipid bilayer density distribution through correlation with these control parameters as future endeavor.

Knowing that two dimensional models have inherent problem of being quantitatively incorrect, we consider this work as

more qualitative. This is a step towards moving to simulate same conditions using three-dimensional models.

The model was used as an attempt to validate the surface tension hypothesis, the physics behind the Fahraeus-Lindqvist effect, and the Fahraeus effect. The simulation is capable of reproducing quiescent erythrocyte biconcave shape and track the deformation of the red blood cell in motion.

The data could be used to calculate blood viscosity in microvessels using variety of models, for example the sigma effect model [16].

REFERENCES

[1] M, M.D., I. Halliday, C.M. Care, and Lyuba Alboul, *Modeling the flow of dense suspensions of defornable particles in three dimensions* PHYSICAL REVIEW E, 2007. **75**: p. 066707-(1-17).

[2] Yaling Liu, W.K.L., *Rheology of red blood cell aggregation by computer simulation.* Journal of Computational Physics, 2006. **220**: p. 139-154.

[3] Krzysztof Boryszko. Witold Dzwinel, a.D.A.Y., *Dynamical Clustering of red blood cells in sapillary vessels.* J Mol Model 2003. **9**(16): p. 16-33.

[4] Ken-ichi TSUBOTA, S.W., and Takami YAMAGUCHI, *Simulation Study on Effects of Hematocrit on Blood Flow Properties Using Particle Method.* Journal of Biomechanical Science and Engineering, 2006. **1**(1): p. 159-170.

[5] BRAASCH, D., *Red Cell Deformability and Capillary Blood Flow.* Physiological Reviews, 1971. **51**(4): p. 679-701.

[6] Ju li, G.l., Ming Dao, and Subra Suresh, *Spectrin-Level Modeling of the Cytoskeleton and Optical Tweezers Stectching of the Erythrocyte* Biophysical Journal 2005. **88**: p. 3707-3719.

[7] Ju li, G.l., Ming Dao, and Subra Suresh, *Cytoskeletal dynamics of human erythrocyte.* PNAS, 2007. **104**(12): p. 4937-4942.

[8] S. L. Keller, W.H.P.I., W.H. Huestis, and H.M. McConnell, *Red Blood Cell Lipids From Immiscible Liquids.* PHYSICAL REVIEW LETTERS, 1998. **81**(22): p. 5019-5022.

[9] Michael C. Sukop, D.T.T., Jr., ed. *Lattice Boltzmann Modeling*. 2007, Springer. 172.

[10] I. Halliday, A.P.H., and C.M. Care, *Lattice Boltzmann algorithm for continuum multicomponent flow.* PHYSICAL REVIEW E, 2007. **76**: p. 026708-(1-13).

[11] M, M.D., I. Halliday, C.M. Care, *Multi-component lattice Boltzmann equation for mesoscale blood flow.* JOURNAL OF PHYSICS A: MATHEMATICAN AND GENERAL, 2003. **36**: p. 8517-8534.

[12] M, M.D., I. Halliday, C.M. Care, *A multi-component Lattice Boltzmann scheme: Towards the mesoscale simulation of blood flow.* Medical Engineering & Physics, 2005. **28 (2006)**: p. 13-18.

[13] H.Rothman, A.K.G.a.D., *Lattice Blotzmann model of immiscible fluids.* PHYSICAL REVIEW A, 1991. **43**(8): p. 4320-4327.

[14] D.Salin, U.D.O.a., *Two-color nonlinear Boltzmann cellular automata: Surface tension and wetting.* PhYSICAL REVIEW E, 1995. **51**(4): p. 3718-3728.

[15] S. V. Lishchuk, C.M.C., and I. Halliday, *Lattice Boltzmann algorithm for surface tension with greatly reduced microcurrents.* PHYSICAL REVIEW E, 2003. **67**: p. 03671-(1-5)

[16] Sun, C. and L. L.Munn, *Particulate Nature of Blood Determines Macroscopic Rheology:A2-D Lattice Boltzmann Analysis.* Biophysical Journal, 2005. **88**: p. 1635-1645.

[17] E.Rittgers, K.B.C.A.P.Y.S., ed. *Biofluid Mechanics. The Human Circulation.* First ed., ed. T. Francis. 2007, A CRC PRESS BOOK: Abingdon, UK. 419.

[18] Ekaterina I Galanzha, V.V.T., Vladimir P Zharov, *Advances in small animal mesentery models for in vivo flow cytometry, dynamic microscopy, and drug screening.* World Journal of Gastroenterology, 2007. **13**(2): p. 192-218.